Characterizing Urban Growth and Peri-Urban Landscape Change in Rondônia using Multiple Endmember Spectral Mixture Analysis

Rebecca Powell[1,2]
Dar Roberts[2]

[1]University of Denver
2050 E. Iliff Ave., Denver, CO 80208, U.S.A.
rpowell8@du.edu

[2]University of California, Santa Barbara
Santa Barbara, CA 93106-4060, U.S.A.
dar@geog.ucsb.edu

Abstract. This study explored the utility of multiple endmember spectral mixture analysis (MESMA) to capture patterns of change in urban and peri-urban land cover through time. MESMA models measured spectra as the linear sum of spectrally pure endmembers and allows endmembers to vary on a per-pixel basis. We analyzed ten urban centers in the state of Rondônia using Landsat TM/ETM+ imagery corresponding to the years 1985, 1990, 1995, and 2000. MESMA was applied to each sample, and two categories of maps were generated: (a) maps of the sub-pixel abundance of generalized urban materials (impervious surfaces, vegetation, and soil), and (b) maps of model complexity (i.e., the number of endmembers required to adequately model each pixel). Model complexity was found to be highly correlated with degree of human impact on the landscape. The relationships between model complexity, urban growth, and changes in the peri-urban landscape were explored in the context of this tropical forest frontier environment.

Keywords: *land-cover change, urban remote sensing, spectral mixture analysis, Amazônia, sensoriamento remoto de áreas urbanas.*

1. Introduction

The state of Rondônia presents a special case for studying urban land-cover change using satellite imagery because the period of rapid settlement and urbanization in the region coincides with the 30-year Landsat data archive (1970s to present). As a result, the trajectory of urbanization in Rondônia has been in large part documented by satellite imagery, a situation that exists in few places in the world.

The most straightforward type of land-cover change involves the conversion of land cover from one class to another, for example forest is replaced by pasture. However, a second, and more subtle, type of change involves modification of land cover, such that the physical properties of the land cover are altered, but the class remains the same, for example degradation of forest by logging activities (Lambin et al., 2003; Yang et al., 2003). In urbanizing landscapes, the first type of change corresponds with urban expansion, the conversion of peri-urban land cover, such as crops or forest, to built-up land cover. The second type of change is characterized by internal modification of urban land-cover, for example, in-filling of open spaces with high-density buildings, paving of roads, regrowth of vegetation, etc. (Rashed et al., 2005).

Most conventional methods of assessing land-cover change only identify transitions between classes, neglecting change within classes due to land-cover modification. This can result in significant error, underestimating the total area experiencing land-cover change, while overestimating the magnitude of change (e.g., Yang et al., 2003). Additionally, identifying change between classes may not be appropriate in an environment where most

change occurs at scales finer than the resolution of the imagery, or where land-cover types are continuous.

This work aims to provide a comprehensive characterization of the urban landscape in terms of physically meaningful, continuous variables using moderate resolution remote sensing imagery. *Spatial* variability of urban environments is addressed by mapping the sub-pixel components of land cover using spectral mixture analysis (SMA), which models each pixel as a linear sum of spectrally 'pure' endmembers (e.g. Adams et al., 1993). *Spectral* variability of urban land cover is addressed by applying multiple endmember spectral mixture analysis (MESMA), a methodology that allows the number and type of endmembers to vary on a per-pixel basis (Roberts et al., 1998b). The products of this work include a set of maps representing the per-pixel fractional cover of the primary components of urban land cover (i.e., vegetation, impervious surfaces, and soil), as well as maps of spectral complexity (i.e., the number of endmembers necessary to model each pixel). The results are locally specific, capturing the spectral variability that is distinct to the region, yet globally representative of urban land cover, allowing comparison of urban composition across regions and through time.

2. Study Area and Data

Ten urban centers in the state of Rondônia were included in this study (**Figure 1**). They were selected to represent a range of populations, development histories, and economic activities. The sample was somewhat biased to cities with larger populations; however, this was deemed necessary because constructing a regional library of impervious spectra required a sufficient number of pixels dominated by built-up land cover.

Figure 1. Study area. Numbered study sites correspond with **Table 1** (below). Sub-scenes centered on each study site, 20-km in each dimension, were extracted from the Landsat TM/ETM+ scenes for further processing.
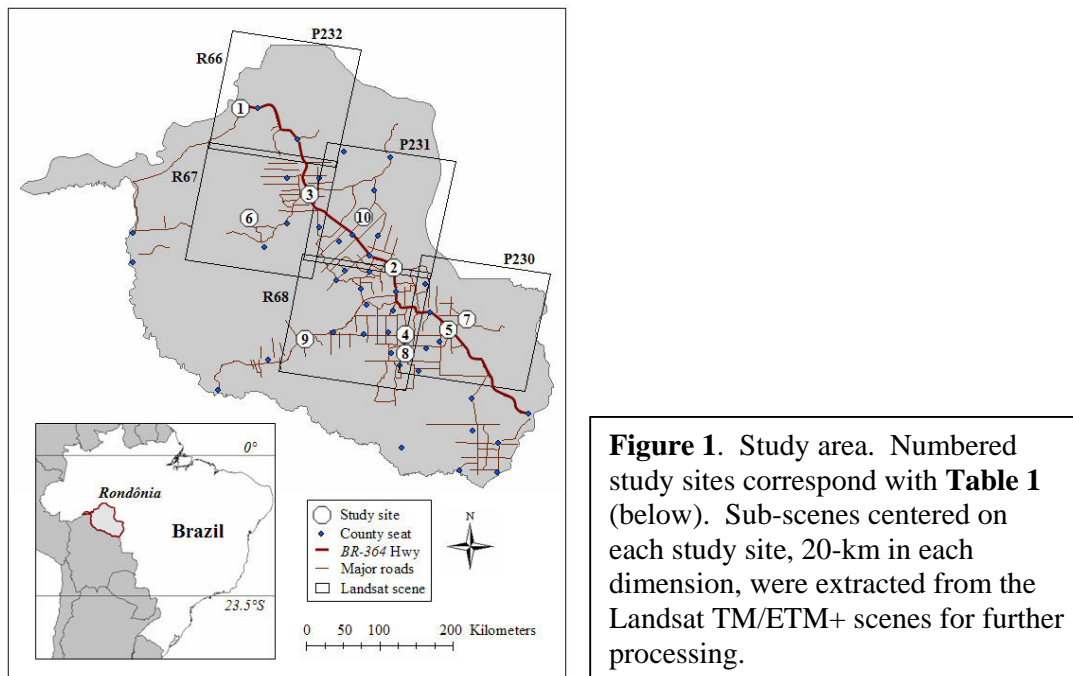
The urban areas were located on five contiguous Landsat scenes. Four sets of Landsat Thematic Mapper (TM) and Landsat Enhanced Thematic Mapper (ETM+) images were selected for each scene to span the time period between 1985 and 2000. Scenes were selected to correspond as closely as possible to the years 1985, 1990, 1995, and 2000, while minimizing cloud cover and haze contamination (**Table 1**). All scenes were co-registered to

1998 or 1999 digital base maps provided by the Instituto Nacional de Pesquisas Espaciais (INPE, 2000). Surface reflectance was derived from 2001 Landsat ETM+ imagery for all scenes using a radiative transfer model as implemented in ACORN software (ImSpec LLC, 2002). Each image in the time series was intercalibrated to its corresponding reflectance image using a relative radiometric calibration approach (Roberts et al., 1998a; Furby and Campbell, 2001). For each urban sample, a region of approximately 400-km^2 (670 x 670 pixels) centered over the built-up area was subset from the reflectance images, and these sub-scenes were the basis of all further analysis.

Table 1. Samples included in the study. The *Reflectance* column refers to the Landsat ETM+ scene used to retrieve apparent surface reflectance. All other dates were intercalibrated to the 2001 reflectance images.

Sample	City	Coordinates	ETM+ scene	Reflectance	2000	1995	1990	1985
1	Porto Velho	8.76S, 63.90W	P232/R66	2001-08-02	2000-06-28	1994-08-07	1989-07-08	1984-07-10
2	Ji-Paraná	10.89S, 61.92W	P231/R67	2001-08-11	2000-08-24	1995-08-03	1990-08-03	1986-10-13
3	Ariquemes	9.91S, 63.03W	P232/R67	2001-08-02	2001-08-02	1996-07-11	1990-08-12	1984-06-24
4	Rolim de Moura	11.72S, 61.78W	P231/R68	2001-08-11	2000-08-24	1995-08-03	1990-08-05	1985-08-07
5	Pimenta Bueno	11.67S, 61.20W	P230/R68	2000-05-29	2001-08-04	1994-08-09	1989-09-12	1984-08-13
6	Buritis	10.21S, 63.83W	P232/R67	2001-08-02	2001-08-02	1996-07-11	1990-08-12	1984-06-24
7	Espigão d'Oeste	11.53S, 61.01W	P230/R68	2000-05-29	2001-08-04	1994-08-09	1989-09-12	1984-08-13
8	Santa Luzia d'Oeste	11.91S, 61.78W	P231/R68	2001-08-11	2000-08-24	1995-08-03	1990-08-05	1985-08-07
9	Seringueiras	11.77S, 63.04W	P231/R68	2001-08-11	2000-08-24	1995-08-03	1990-08-05	1985-08-07
10	Theobroma	10.25S, 62.35W	P231/R67	2001-08-11	2000-08-24	1995-08-03	1990-08-03	1986-10-13

Reference data were produced from digital aerial videography collected over the region on June 22, 1999, as part of the Validation Overflights for Amazon Mosaics (Hess et al., 2002). The flight lines transected three of the urban areas in the sample: Ji-Paraná, Rolim de Moura, and Santa Luzia d'Oeste. Average swath width for videography in zoom mode was 65 m, with an average ground instantaneous field of view (GIFOV) of approximately 0.3 m. On June 22, the global positioning system (GPS) was not functioning properly, and therefore georeferencing was not recorded as the data were collected. Nonetheless, it was still possible to estimate aircraft height and to generate free-standing mosaics, which were in turn manually georeferenced to the Landsat images.

3. Methods

Multiple endmember spectral mixture analysis (MESMA) was applied to each sub-scene (Roberts et al., 1998b). First, an endmember library was constructed from candidate image and reference endmembers. Then, a series of simple SMA models based on different combinations of library endmembers was applied to every pixel in the image, and the 'best-fit' model was selected for each pixel. The models were generalized into the land-cover components of interest (i.e., vegetation, impervious surface, soil), and an image of per-pixel fractional coverage was generated for each component. How well the fraction images represented the actual fractions of each land-cover component was assessed by comparing the modeled fractions to fractional cover measured from classified aerial videography. Agreement between modeled fraction cover and reference fraction cover was used to refine the combinations of endmembers allowed for SMA modeling, as well as to select to most appropriate constraints and model selection rules. The procedure for applying MESMA to multispectral imagery is detailed in Powell et al. (2006).

The final product of this analysis was a set of fractional abundance maps for each class of materials (i.e. vegetation, impervious surfaces, soil). Because shade was not considered a land-cover component, but rather a variant on endmember brightness, the fractions of each pixel were shade-normalized (Adams et al., 1993). For two-endmember models, the resulting

shade-normalized fraction was 100%. After shade normalization, the endmembers were relabeled as their corresponding generalized class; green vegetation and non-photosynthetic vegetation (NPV) were combined into a single vegetation class. These shade-normalized, class-generalized fractions were combined to generate an image of each land-cover material, with values representing the physical abundance of that material.

4. Results

4.1 Summary

Two complementary products resulted from the application of MESMA to the Rondônia time series. First were maps of the sub-pixel fractions that characterize the landscape with continuous, physically based variables. These variables could be used as input to thematic image classification (e.g. Roberts et al., 2002); however, the fractions provide spatially explicit information in terms of degree and direction of land-cover change that would not be available if they were converted to thematic classes (Rashed et al., 2005; Yang et al., 2003). The second product that resulted from application of MESMA was a measure of spectral complexity, as represented by the number of endmembers required to adequately model each pixel. This measure of spectral complexity was correlated with the degree of human impact on the landscape.

When the results for all ten study-sites across all four dates were assessed in aggregate, 97.6% of all pixels were successfully modeled by MESMA or classified as water or burn scar. The pixels that remained unmodeled tended to fall in two categories: (1) edge pixels, particularly between land and water or between land-cover types with distinctly different geometries, e.g. pasture and primary forest, and (2) heavily shadowed pixels located in primary forest.

4.2 Accuracy Assessment

Accuracy measures were based on the correlation between modeled fractions and reference fractions derived from the aerial videography. The 'accuracy' of modeled fractions was assessed by the slope, intercept, and R-squared values associated with the relationship. In an ideal case, when the modeled data perfectly represents the reference data, the slope of the relationship would equal one, the intercept zero, and the R^2 value would approach one. Two types of error measurement were also used to evaluate the range of disagreement between fraction estimates: mean absolute error and bias. Mean absolute error (MAE) is the average absolute value of the difference between modeled and measured fraction values, while bias is the average of the error, indicating general trends in over- or under-estimation (Schwarz and Zimmermann, 2005).

Table 2. Summary measures for accuracy assessment. *RSQ* refers to R-squared; *MAE* to mean absolute error. A total of 41 samples were included.

	Veg	Imp	Soil
slope	0.787	0.814	0.704
intercept	10.75	5.99	5.99
RSQ	0.858	0.759	0.710
MAE	7.71	5.55	8.59
Bias	1.71	2.99	-6.20

Correlation between modeled fractions and reference fractions was highest for impervious fractions and lowest for soil fractions (**Table 2**). The vegetation fraction had a relatively high

slope (0.787) and the highest correlation (0.858). For all classes, the intercept was approximately 10% or lower, and the mean absolute error was also less than 10%. The biases for all classes were quite low (**Table 2**). The impervious and vegetation fractions had very small, positive biases (below 3%), indicating a slight over-estimation of the modeled fractions relative to the reference fractions. The soil fractions had a slightly larger negative bias (approximately 6%), indicating a general trend of underestimation of the soil fractions.

4.3 Mapping Urban Extent

Based on visual inspection, the spatial patterns of the predicted impervious fractions appeared reasonable; that is, for all study samples, the extent of built-up land cover was captured by the distribution of pixels modeled with an impervious surface spectrum, and conversely, very little of the 'hinterland' was modeled with impervious fractions. In addition to capturing urban extent, maps of impervious surface fractions provide spatially explicit information concerning the direction and magnitude of change in built-up land cover (Rashed et al., 2005; Yang et al., 2003). **Figure 2** presents the estimated impervious surface fractions for one of the study areas—Buritis—at two points in time. Buritis was the youngest and most rapidly growing settlements among the study sites.

Maps of impervious fractions for Buritis demonstrate change in urban extent and change in urban composition. The 1990 image of Buritis (not presented) consisted of *terra firme* forest dotted with very small plots of cleared land, and as a result, no pixels in the sub-scene were modeled with impervious fractions. A comparison of Buritis in 1996 and 2001 (**Figure 2**) clearly illustrates the expansion of the settlement through time. There was also an increase in the density of built-up surfaces. Within the area mapped as built-up in 1996, there was considerable in-filling of pixels modeled with impervious spectra, and for pixels modeled with impervious spectra in 1996, there was also an increase in the fraction of impervious surfaces.
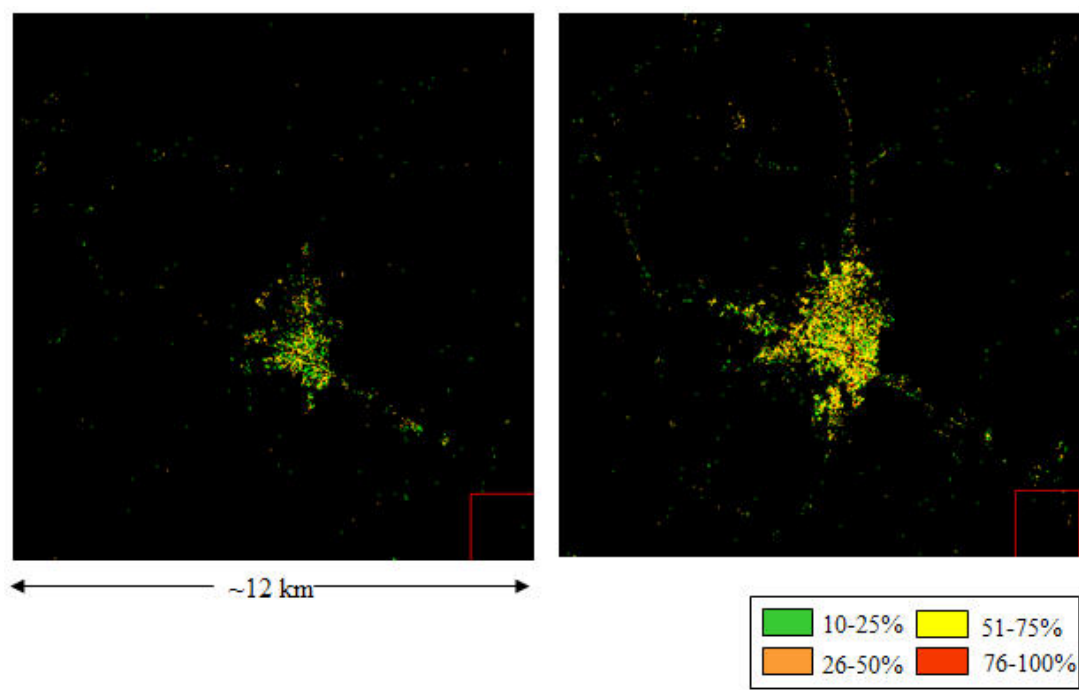
Figure 2. Maps of percent impervious cover for Buritis in 1996 (*left*) and 2001 (*right*). Black pixels have an impervious fraction of zero.

4.4 Characterizing peri-urban land-cover change

The number of endmembers required to adequately model each pixel was found to be correlated with the degree of human impact on the landscape, a factor that is expected to vary spatially and temporally. Four-endmember models are associated with built-up land cover, and therefore the percentage of four-endmember models in a given area is expected to decrease with distance from the urban center. Three-endmember models are associated with human-modified land-cover types, such as pasture and second-growth vegetation. Land immediately surrounding the urban center is expected to have a high percentage of pixels modeled by three-endmembers, a percentage expected to decrease with distance from the urban center, as human impact diminishes. Two-endmember models are associated with natural land cover, such as primary forest or natural savanna, and the percentage of two-endmember models is generally expected to increase with distance from urban center.

Similar variations occur through time: the percentage of two-endmember models is expected to decrease through time, as land is cleared for pasture, crops, or urban expansion; and the percentage of three-endmember models is expected to increase with time, as human impact on the landscape extends further from the original settlement. The rate of decrease of two-endmember models and corresponding increase of three-endmember models is correlated with the rate of land-cover conversion.
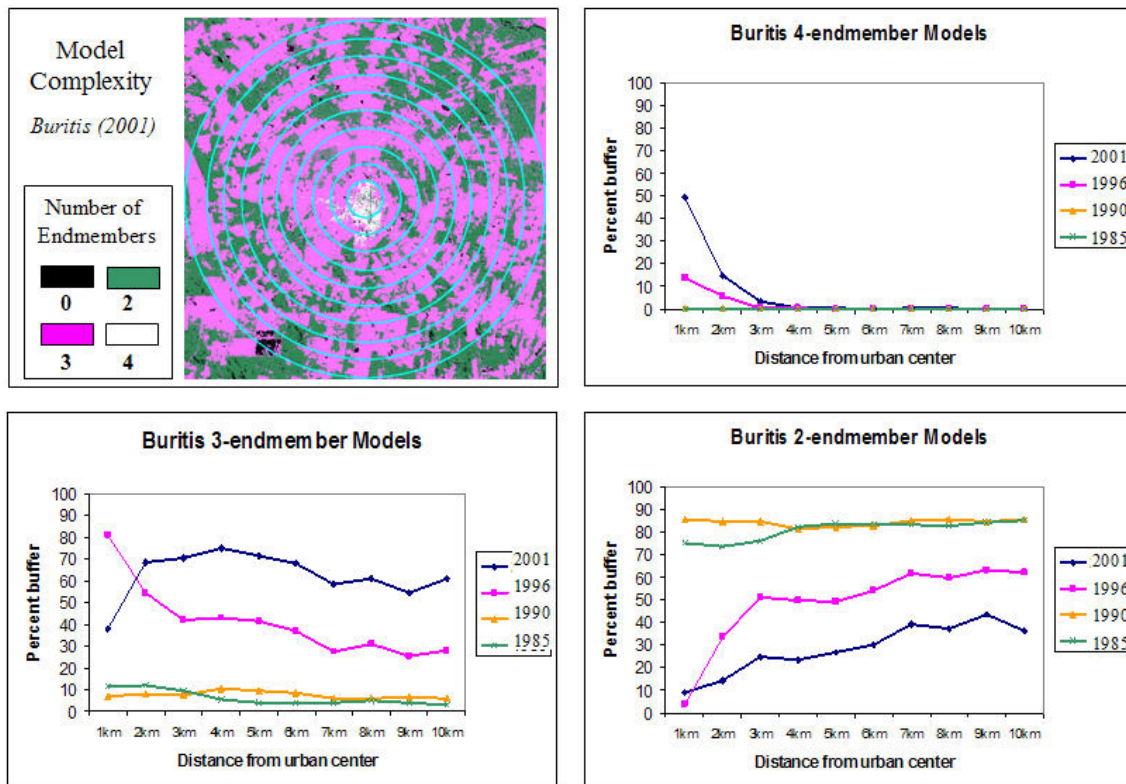
Figure 3. One-kilometer buffers overlaid on the 2001 map of model complexity for Buritis. Water, burned, and unmodeled pixels are black. (*Upper left*). Summaries of model complexity for Buritis as a function of distance from the urban center and as a function of time: Four-endmember models (*upper right*), three-endmember models (*lower left*), and two-endmember models (*lower right*). Numbers are reported as a percent of the buffer area for each distance from the urban center.

In this context, we explored the relationships between model complexity, urban growth, and changes in the peri-urban landscape. Building on the work of Boucek and Moran (2004), concentric one-kilometer buffers were overlaid on the sub-images, and the percent of each buffer area composed of two-, three-, and four-endmember models was calculated (**Figure 3**). Trends in the degree of human impact as a function of distance from the urban center and as a function of time were compared. In general, the expected patterns described above occurred at every site within the study, but variations in such patterns indicate variations in settlement histories and in the human activities driving land-cover conversion. The example of Buritis is presented in **Figure 3**.

The city of Buritis represents an extreme example of urbanization on the landscape, because in 1990 the city did not exist and the landscape consisted almost entirely of *terra firme* forest, with only tiny patches of cleared forest. By 1995, roads cut across the landscape, much of the adjacent forest had been cleared, and a substantial settlement had emerged. These patterns are reflected in maps of model complexity, such as that presented in **Figure 3**, and are quantified in graphs of endmember complexity as a function of distance from the urban center. For the earliest two dates in the time series (1985 and 1990), there were no four-endmember models, indicating there was no urban/built-up land cover in the scene. Close to 90% of the landscape for those dates was composed of two-endmember models, indicating very little, if any, human impact in the area and that almost all of the original forest remained intact. In 1996, four-endmember models have appeared at urban core (~15% of the 1-km buffer zone), and by 2001, four-endmember models composed almost 50% of 1-km urban buffer zone, indicating rapid increase of urban/built-up land cover. The 1996 and 2001 images also resulted in dramatic but steady decrease in the percentage of two-endmember models and increase in the percentage of three-endmember models, indicating a trend of increasing conversion of forest to pasture and/or crops.

5. Discussion

This work has demonstrated that MESMA can be applied to a regional time series using the same endmember library, the same model constraints and selection rules, for all dates in the time series. Additionally, information provided by the time series in an urban environment allowed refinement of the MESMA endmember library and model selection rules without additional reference data. This is because impervious materials were expected to be spatially constrained, with probabilities diminishing as a function of distance from the urban center, and the area covered by impervious materials was expected to be temporally consistent, increasing or remaining constant through time. These factors increased confidence in the resulting maps of sub-pixel impervious fractions.

A potential limitation of MESMA application for change detection emerged in this study; that is the effect of atmospheric variation on model selection. While achieving radiometric consistency between dates is a well-acknowledged challenge for any time-series analysis using remote sensing data (e.g., Roberts et al., 1998a), the results of this study indicate that the problem may become particularly pronounced when MESMA is applied. This is in part related to the limited dimensionality of Landsat TM data, which in turn restricts spectral separability between some material classes. A high rate of model degeneracy can result, as a large numbers of pixels can be represented by more than one model within the MESMA constraints. Which model was selected as best representing each pixel could switch based on relatively minor differences in measured reflectance.

Finally, this work has presented a preliminary analysis of model complexity as a function of distance from the urban center and as a function of time. Model complexity provides a simple measure of the spectral complexity of each pixel and is correlated with the degree of

human impact on the landscape. Several simplifications may limit the scope of the analysis presented here. For example, the 1-km buffers used for analysis arbitrarily divide the landscape into units that neither correspond to physical nor social phenomena. In addition, each buffer corresponds to a different area, potentially limiting comparability between buffer regions (Boucek and Moran, 2004). However, even given these simplifications, this work has demonstrated the possibility of quantifying relationships between land-cover change and urbanization. Such an analysis provides a first step in linking socio-economic drivers of land-cover change to specific patterns on the peri-urban landscape. These links could contribute to developing a more comprehensive story to explain the emergence of different patterns and rates of land-cover change on the frontier and their relationship to urbanization.

References

Adams, J. B.; Smith, M. O.; Johnson, P. E. Imaging spectroscopy: interpretation based on spectral mixture analysis. In C. M. Pieters; P. A. J. Englert (Eds.). **Remote Geochemical Analysis: Elemental and Mineralogical Composition**. Cambridge, England: Cambridge University Press, 1993, p. 145-164.

Boucek, B.; Moran, E. F. Inferring the behavior of households from remotely sensed changes in land cover: Current methods and future directions. In M.F. Goodchild; D.G. Janelle (Eds.). **Spatially Integrated Social Science**. Oxford, England: Oxford University Press, 2004, p. 23-47.

Furby, S. L.; Campbell, N. A. Calibrating images from different dates to 'like-value' digital counts. **Remote Sensing of Environment**, v. 77, p. 186-196, 2001.

Hess, L. L.; Novo, E. M. L. M.; Slaymaker, D. M.; Holt, J.; Steffen, C.; Valeriano, D. M.; Mertes, L. A. K.; Krug, T.; Melack, J. M.; Gastil, M.; Holmes, C.; Hayward, C. Geocoded digital videography for validation of land cover mapping in the Amazon basin. **International Journal of Remote Sensing**, v. 23, p. 1527-1556, 2002.

ImSpec LLC. **ACORN 4.0 User's Guide**. Boulder, Colorado: Analytical Imaging and Geophysics LLC, 2002, 76 p.

INPE. **Monitoramento da floresta Amazônica Brasileira por Satéllite 1998-1999**. São José dos Campos: Instituto Nacional de Pesquisas Espacias, 2000, 22 p.

Lambin, E. F.; Geist, H. J.; Lepers, E. Dynamics of land-use and land-cover change in tropical regions. **Annual Review of Environment and Resources**, v. 28, p. 205-241, 2003.

Powell, R. L.; Roberts, D. A.; Dennison, P. E.; Hess, L. L. Sub-pixel mapping of urban land cover using multiple endmember spectral mixture analysis: Manaus, Brazil. **Remote Sensing of Environment**, *In Press*, 2006.

Rashed, T.; Weeks, J. R.; Stow, D.; Fugate, D. Measuring temporal compositions of urban morphology through spectral mixture analysis: towards a soft approach to change analysis in crowded cities. **International Journal of Remote Sensing**, v. 26, p. 699-718, 2005.

Roberts, D. A.; Batista, G. T.; Pereira, L. G.; Waller, E. K.; Nelson, B. W. Change identification using multitemporal spectral mixture analysis: applications in Eastern Amazonia. In R. S. Lunetta; C. D. Elvidge (Eds). **Remote Sensing Change Detection: Environmental Monitoring Methods and Applications**. Chelsea, Michigan: Ann Arbor Press, 1998a, p. 137-161.

Roberts, D. A.; Gardner, M.; Church, R.; Ustin, S.; Scheer, G.; Green, R. O. Mapping chaparral in the Santa Monica Mountains using multiple endmember spectral mixture models. **Remote Sensing of Environment**, v. 65, p. 267-279, 1998b.

Roberts, D. A.; Numata, I.; Holmes, K.; Batista, G; Krug, T; Moteiro, A.; Powell, B.; Chadwick, O. A. Large area mapping of land-cover change in Rondônia using multispectral spectral mixture analysis and decision-tree classifiers. **Journal of Geophysical Research—Atomospheres**, v. 107, n. 8073, p. LBA 40.1-40.18, 2002.

Schwarz, M.; Zimmermann, N. E. A new GLM-based method for mapping tree cover continuous fields using regional MODIS reflectance data. **Remote Sensing of Environment**, v. 95, p. 428-443, 2005.

Yang, L.; Xian, G.; Klaver, J. M.; Deal, B. Urban land-cover change detection through sub-pixel imperviousness mapping using remotely sensed data. **Photogrammetric Engineering and Remote Sensing**, v. 69, p. 1003-1010, 2003.